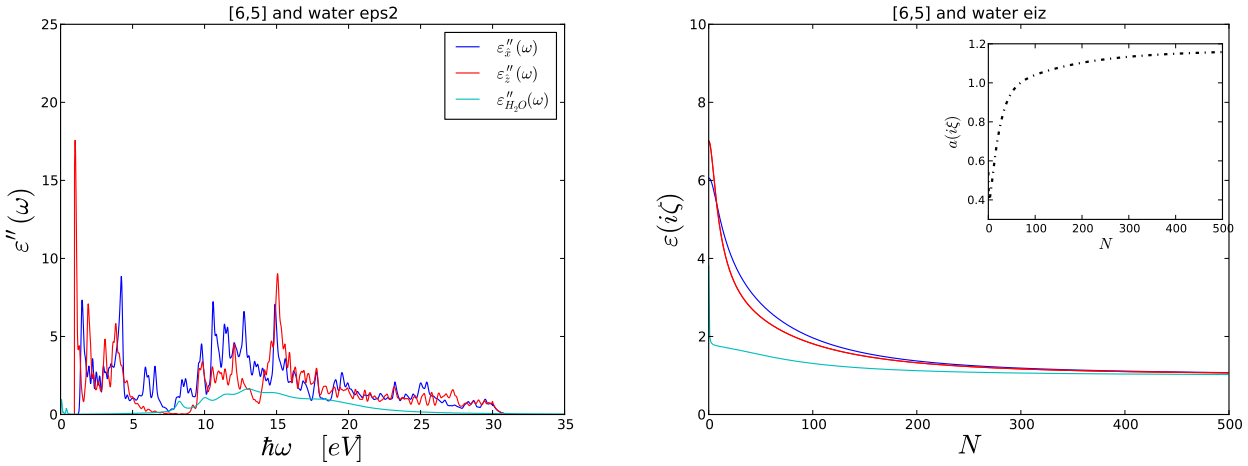

(a) (b)

FIG. 1: Full result using Eqs.5,6 (a) Anisotropic response functions for CG-10 DNA and water. The DNA response functions in the x and y directions were used as perpendicular and parallel inputs, respectively. CG-10 and water eps2 data was provided by Dan Dryden. CG-10 data scales Wai-Yim's calculations by 4.94 and is assumed to include Na (more info in Dan Dryden email sent to us on Nov. 8, 2013). Water data was built from lorentz oscillators R.H.French,J.Amer.Ceram Soc.,83,9,2117-46(2000), H.D.Ackler, et al,J.Coll.Interface Sci.179,46. (b) Anisotropy metric $a_{1,2}(i\zeta_n)$ using Eq.12, compares the anisotropy of the cylinders (DNA) to their intervening material, water for the terms contruting to the Matsubara sum.

Hamaker coefficents for two identical anisotropic cylinder at all separations A comparison of Gecko Hamaker and Python results

J. Hopkins

Dan sent some data, I made A's. He generated A's from GH. I plotted both results for comparison. They should agree. They don't.

I. IMAGINARY PART OF THE DIELECTRIC RESPONSE FUNCTION AND ANISOTROPY METRIC

The dielectric response functions are evaluated at imaginary frequencies, thus $\epsilon_{\parallel,\perp} = \epsilon_{\parallel,\perp}(i\omega)$. $\epsilon_{\parallel,\perp}(i\omega)$ is referred to as the London - van der Waals transform of the response function $\epsilon_{\parallel,\perp}(\omega)$ and is given by the Kramers - Kronig relations. It is strictly a real, monotonically decaying function of ω.

II. ANISOTROPY METRIC

The ratios between the relative anisotropy measures (Eq. **??**) defined as

$$a = \frac{2\Delta_\perp}{\Delta_\parallel} = 2\frac{(\epsilon^c{}_\perp - \epsilon_m)\epsilon_m}{(\epsilon^c{}_\perp + \epsilon_m)(\epsilon^c{}_\parallel - \epsilon_m)} \tag{1}$$

and is obviously frequency dependent. Parameters a_1 and a_2 can be thought of as a specific measure of the anisotropy of the cylinders in the left and right half-spaces when compared with the isotropic bathing medium m. Note that they vanish when the transverse dielectric response of the cylinder material equals the medium response. The explicit form of the second derivative of $f(\ell, \theta)$ now follows as

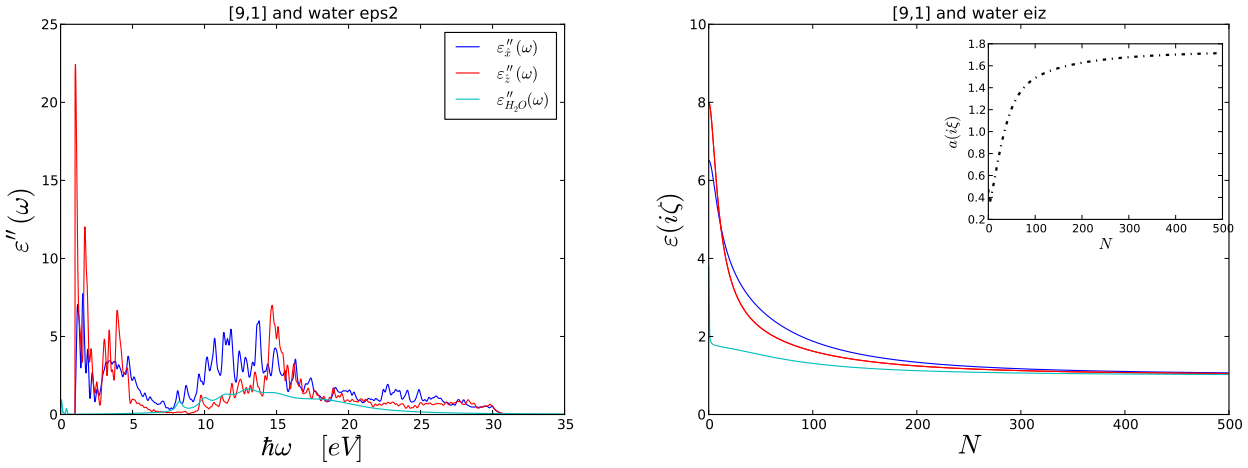

(a) (b)

FIG. 2: Full result using Eqs.5,6 (a) Anisotropic response functions for CG-10 DNA and water. The DNA response functions in the x and y directions were used as perpendicular and parallel inputs, respectively. CG-10 and water eps2 data was provided by Dan Dryden. CG-10 data scales Wai-Yim's calculations by 4.94 and is assumed to include Na (more info in Dan Dryden email sent to us on Nov. 8, 2013). Water data was built from lorentz oscillators R.H.French,J.Amer.Ceram Soc.,83,9,2117-46(2000), H.D.Ackler, et al,J.Coll.Interface Sci.179,46. (b) Anisotropy metric $a_{1,2}(i\zeta_n)$ using Eq.12, compares the anisotropy of the cylinders (DNA) to their intervening material, water for the terms contruting to the Matsubara sum.

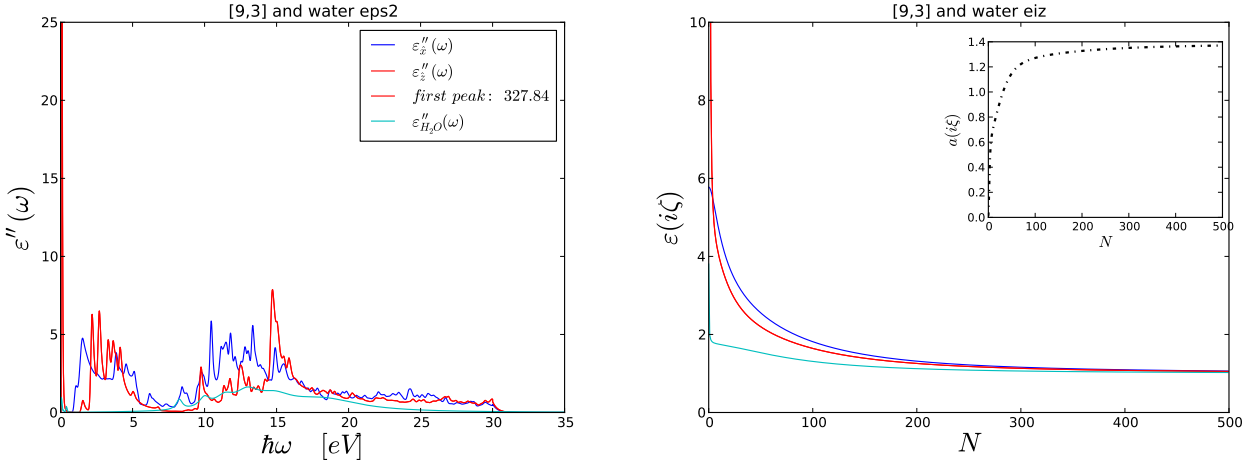

(a) (b)

FIG. 3: Full result using Eqs.5,6 (a) Anisotropic response functions for CG-10 DNA and water. The DNA response functions in the x and y directions were used as perpendicular and parallel inputs, respectively. CG-10 and water eps2 data was provided by Dan Dryden. CG-10 data scales Wai-Yim's calculations by 4.94 and is assumed to include Na (more info in Dan Dryden email sent to us on Nov. 8, 2013). Water data was built from lorentz oscillators R.H.French,J.Amer.Ceram Soc.,83,9,2117-46(2000), H.D.Ackler, et al,J.Coll.Interface Sci.179,46. (b) Anisotropy metric $a_{1,2}(i\zeta_n)$ using Eq.12, compares the anisotropy of the cylinders (DNA) to their intervening material, water for the terms contruting to the Matsubara sum.

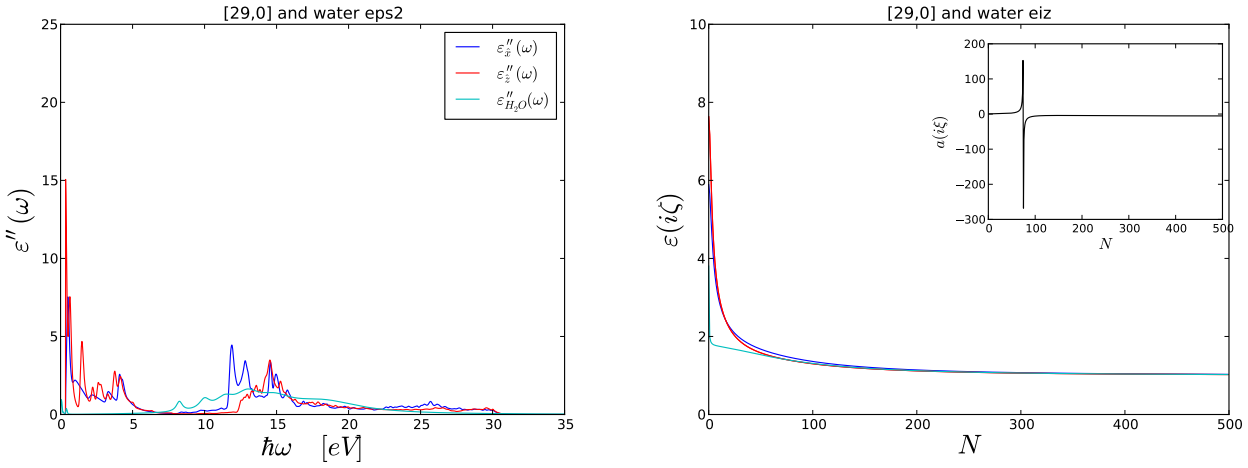

(a) (b)

FIG. 4: Full result using Eqs.5,6 (a) Anisotropic response functions for CG-10 DNA and water. The DNA response functions in the x and y directions were used as perpendicular and parallel inputs, respectively. CG-10 and water eps2 data was provided by Dan Dryden. CG-10 data scales Wai-Yim's calculations by 4.94 and is assumed to include Na (more info in Dan Dryden email sent to us on Nov. 8, 2013). Water data was built from lorentz oscillators R.H.French,J.Amer.Ceram Soc.,83,9,2117-46(2000), H.D.Ackler, et al,J.Coll.Interface Sci.179,46. (b) Anisotropy metric $a_{1,2}(i\zeta_n)$ using Eq.12, compares the anisotropy of the cylinders (DNA) to their intervening material, water for the terms contruting to the Matsubara sum.

$$\frac{d^2 f(\ell,\theta)}{d\ell^2} = -\frac{v_1 v_2 \Delta_{1,\parallel}\Delta_{2,\parallel}}{32}\frac{e^{-2\ell\sqrt{Q^2+\epsilon_m\frac{\omega_n^2}{c^2}}}}{(Q^2+\epsilon_m\frac{\omega_n^2}{c^2})} \left\{2\left[(1+3a_1)(1+3a_2)Q^4 + 2(1+2a_1+2a_2+3a_1a_2)Q^2\epsilon_m\frac{\omega_n^2}{c^2} + 2(1+a_1)(1+a_2){\epsilon_m}^2\frac{\omega_n^4}{c^4}\right] + \right. \left. + (1-a_1)(1-a_2)\left(Q^2+2\epsilon_m\frac{\omega_n^2}{c^2}\right)^2\cos 2\theta\right\}. \quad (2)$$

Here R_1 and R_2 are the cylinder radii, assumed to be the smallest lengths in the problem [**?**]. The frequency dependence of the dielectric functions is in $\epsilon_m(i\omega_n)$, ${\epsilon^c}_\perp(i\omega_n)$ and ${\epsilon^c}_\parallel(i\omega_n)$, and therefore also $a = a(i\omega_n)$. The frequencies in the Matsubara summation are $\omega_n = 2\pi\ \frac{k_B T}{\hbar}n$. Note that Eq. 2 is symmetric with respect to 1 and 2 indices (left and right half-spaces), as it should be.

III. PERPENDICULAR CYLINDERS

A. Fully retarded

We use Eq. **??** to obtain the interaction free energy between two skewed cylinders:

$$G(\ell,\theta) = -\frac{k_B T}{64\pi}\frac{\pi^2 R_1^2 R_2^2}{\ell^4\sin\theta}{\sum_{n=0}^{\infty}}' \Delta_{1,\parallel}\Delta_{2,\parallel}\int_0^\infty udu\ \frac{e^{-2\sqrt{u^2+p_n^2}}}{(u^2+p_n^2)}g(a_1,a_2,u,p_n,\theta), \quad (3)$$

where $u = Q\ell$,

$$g(a_1,a_2,u,p_n,\theta) = 2\left[(1+3a_1)(1+3a_2)u^4 + 2(1+2a_1+2a_2+3a_1a_2)u^2p_n^2 + 2(1+a_1)(1+a_2)p_n^4\right] + + (1-a_1)(1-a_2)(u^2+2p_n^2)^2\cos 2\theta \quad (4)$$

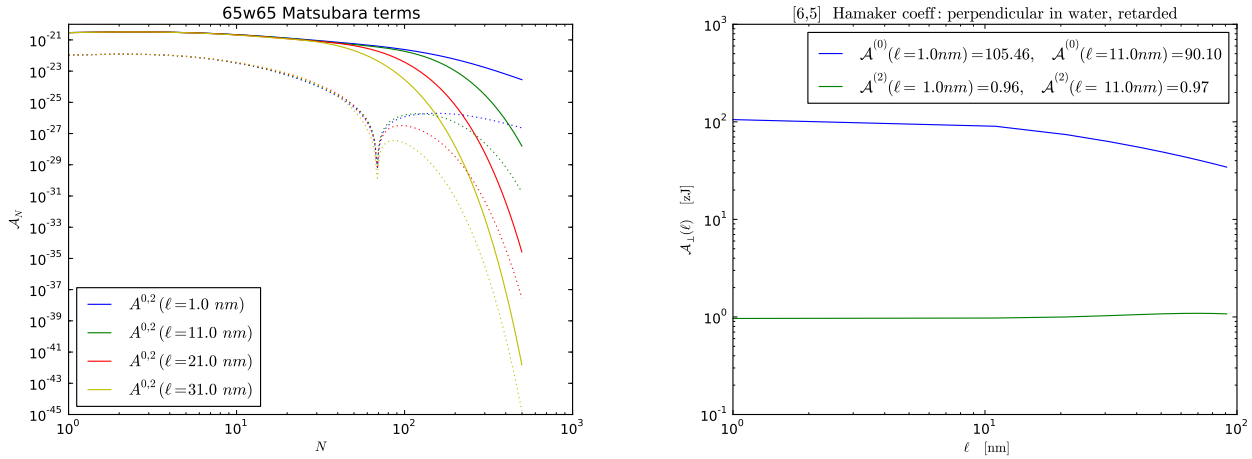

(a) (b)

FIG. 5: Full result using Eqs.5,6 (a) Anisotropic response functions for CG-10 DNA and water. The DNA response functions in the x and y directions were used as perpendicular and parallel inputs, respectively. CG-10 and water eps2 data was provided by Dan Dryden. CG-10 data scales Wai-Yim's calculations by 4.94 and is assumed to include Na (more info in Dan Dryden email sent to us on Nov. 8, 2013). Water data was built from lorentz oscillators R.H.French,J.Amer.Ceram Soc.,83,9,2117-46(2000), H.D.Ackler, et al,J.Coll.Interface Sci.179,46. (b) Anisotropy metric $a_{1,2}(i\zeta_n)$ using Eq.12, compares the anisotropy of the cylinders (DNA) to their intervening material, water for the terms contruting to the Matsubara sum.

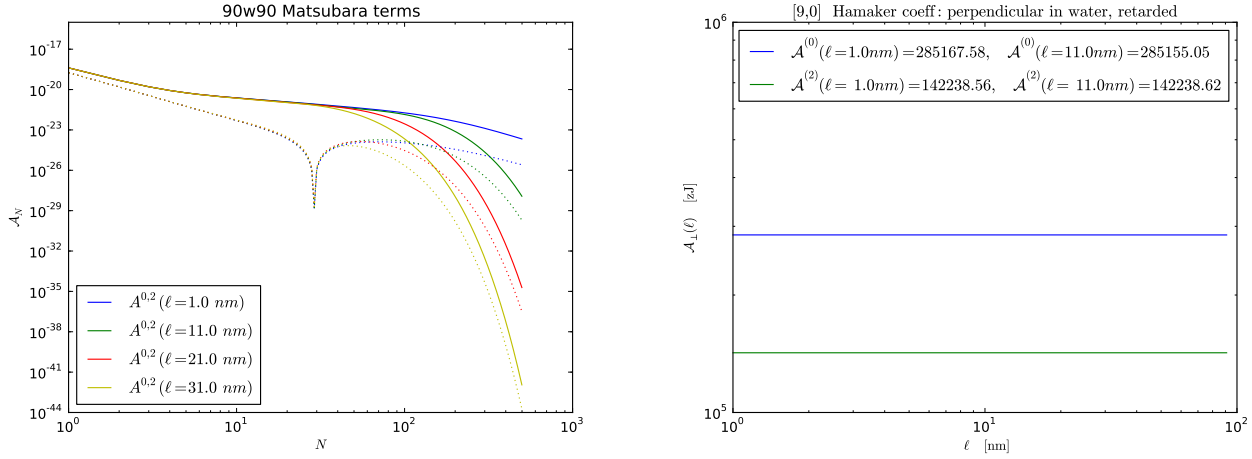

(a) (b)

FIG. 6: Full result using Eqs.5,6 (a) Anisotropic response functions for CG-10 DNA and water. The DNA response functions in the x and y directions were used as perpendicular and parallel inputs, respectively. CG-10 and water eps2 data was provided by Dan Dryden. CG-10 data scales Wai-Yim's calculations by 4.94 and is assumed to include Na (more info in Dan Dryden email sent to us on Nov. 8, 2013). Water data was built from lorentz oscillators R.H.French,J.Amer.Ceram Soc.,83,9,2117-46(2000), H.D.Ackler, et al,J.Coll.Interface Sci.179,46. (b) Anisotropy metric $a_{1,2}(i\zeta_n)$ using Eq.12, compares the anisotropy of the cylinders (DNA) to their intervening material, water for the terms contruting to the Matsubara sum.

and $p_n^2(\ell)=\epsilon_m(i\omega_n)\frac{\omega_n^2}{c^2}\ell^2$. Another change of variables with $u=p_n t$, yields

$$G(\ell,\theta)=-\frac{k_BT}{64\pi}\frac{\pi^2R_1^2R_2^2}{\ell^4\sin\theta}{\sum_{n=0}^{\infty}}'\Delta_{1,\parallel}\Delta_{2,\parallel}\ p_n^4\ \int_0^\infty tdt\ \frac{e^{-2p_n\sqrt{t^2+1}}}{(t^2+1)}\tilde{g}(t,a_1(i\omega_n),a_2(i\omega_n),\theta), \tag{5}$$

with

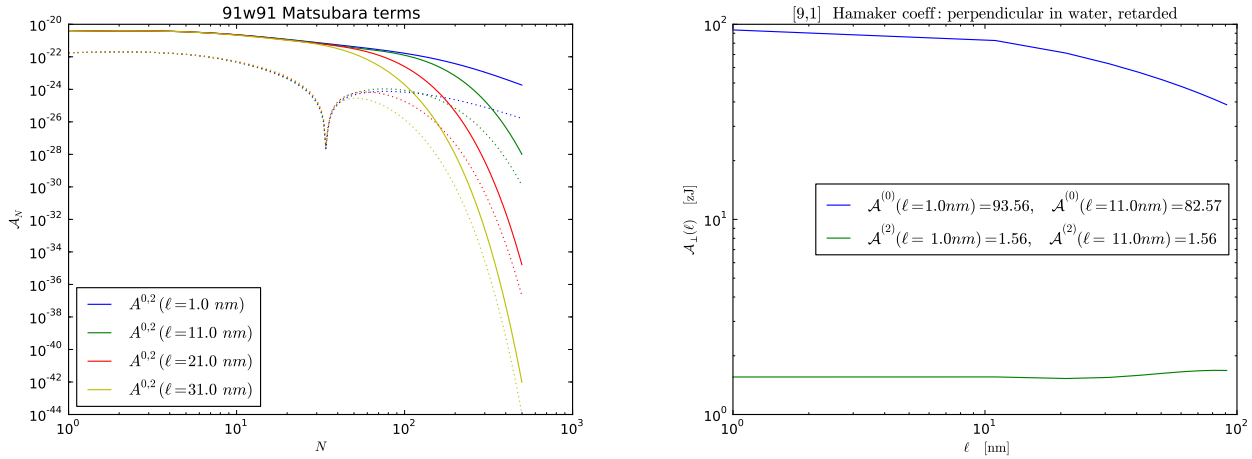

(a) (b)

FIG. 7: Full result using Eqs.5,6 (a) Anisotropic response functions for CG-10 DNA and water. The DNA response functions in the x and y directions were used as perpendicular and parallel inputs, respectively. CG-10 and water eps2 data was provided by Dan Dryden. CG-10 data scales Wai-Yim's calculations by 4.94 and is assumed to include Na (more info in Dan Dryden email sent to us on Nov. 8, 2013). Water data was built from lorentz oscillators R.H.French,J.Amer.Ceram Soc.,83,9,2117-46(2000), H.D.Ackler, et al,J.Coll.Interface Sci.179,46. (b) Anisotropy metric $a_{1,2}(i\zeta_n)$ using Eq.12, compares the anisotropy of the cylinders (DNA) to their intervening material, water for the terms contruting to the Matsubara sum.

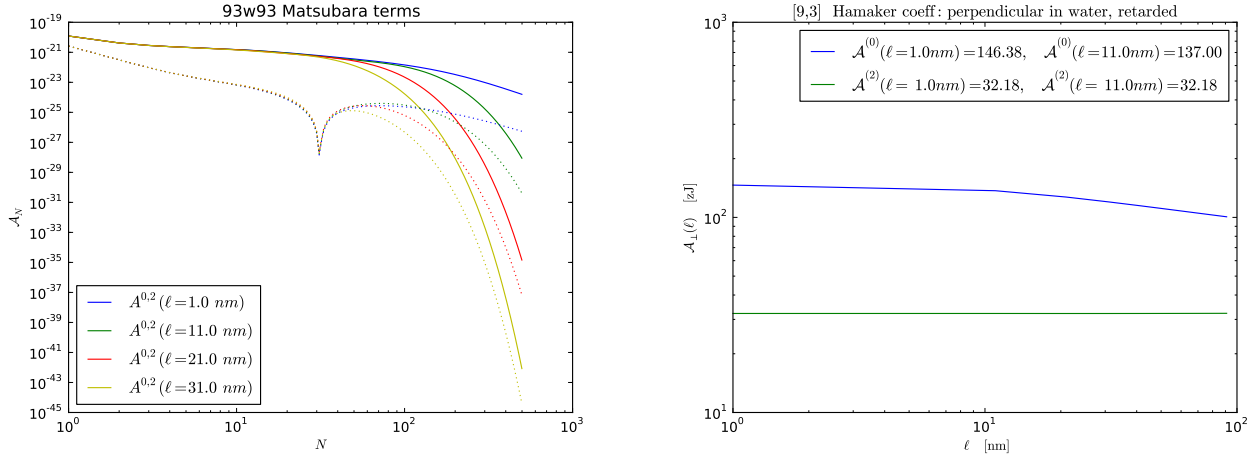

(a) (b)

FIG. 8: Full result using Eqs.5,6 (a) Anisotropic response functions for CG-10 DNA and water. The DNA response functions in the x and y directions were used as perpendicular and parallel inputs, respectively. CG-10 and water eps2 data was provided by Dan Dryden. CG-10 data scales Wai-Yim's calculations by 4.94 and is assumed to include Na (more info in Dan Dryden email sent to us on Nov. 8, 2013). Water data was built from lorentz oscillators R.H.French,J.Amer.Ceram Soc.,83,9,2117-46(2000), H.D.Ackler, et al,J.Coll.Interface Sci.179,46. (b) Anisotropy metric $a_{1,2}(i\zeta_n)$ using Eq.12, compares the anisotropy of the cylinders (DNA) to their intervening material, water for the terms contruting to the Matsubara sum.

$$\tilde{g}(t,a_1,a_2,\theta) \;=\; 2\left[(1+3a_1)(1+3a_2)t^4+2(1+2a_1+2a_2+3a_1a_2)t^2+2(1+a_1)(1+a_2)\right]+ \\ +(1-a_1)(1-a_2)(t^2+2)^2\cos 2\theta. \qquad (6)$$

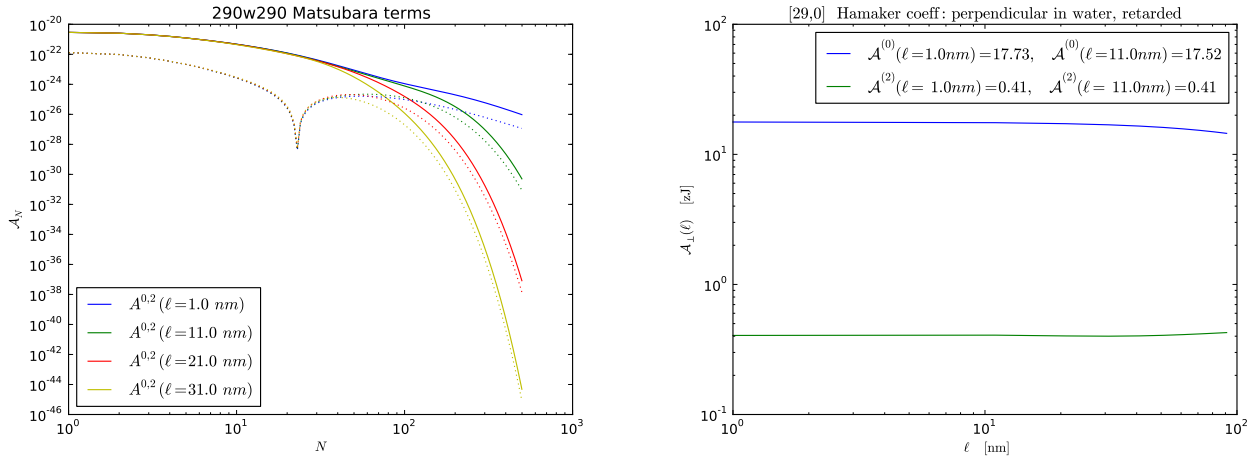

(a) (b)

FIG. 9: Full result using Eqs.5,6 (a) Anisotropic response functions for CG-10 DNA and water. The DNA response functions in the x and y directions were used as perpendicular and parallel inputs, respectively. CG-10 and water eps2 data was provided by Dan Dryden. CG-10 data scales Wai-Yim's calculations by 4.94 and is assumed to include Na (more info in Dan Dryden email sent to us on Nov. 8, 2013). Water data was built from lorentz oscillators R.H.French,J.Amer.Ceram Soc.,83,9,2117-46(2000), H.D.Ackler, et al,J.Coll.Interface Sci.179,46. (b) Anisotropy metric $a_{1,2}(i\zeta_n)$ using Eq.12, compares the anisotropy of the cylinders (DNA) to their intervening material, water for the terms contruting to the Matsubara sum.

The cylinder-cylinder interaction at all angles when the radii of the cylinders are the smallest lengths in the system. It includes retardation and the full angular dependence:

$$\boxed{G(\ell,\theta)=-\frac{(\pi R_1^2)(\pi R_2^2)}{2\pi\ \ell^4\sin\theta}\left(\mathcal{A}^{(0)}(\ell)+\mathcal{A}^{(2)}(\ell)\cos 2\theta\right),} \tag{7}$$

Where (ℓ) is the inter surface separation. The (ℓ) dependence of the Hamaker coefficients $\mathcal{A}$ is a consequence of (ℓ) dependence of $p_n^2(\ell)=\epsilon_m(i\omega_n)\frac{\omega_n^2}{c^2}\ell^2$. Above we defined

$$\mathcal{A}^{(0)}(\ell)=\frac{k_BT}{32}{\sum_{n=0}^{\infty}}'\Delta_{1,\|}\Delta_{2,\|}\ p_n^4(\ell)\ \int_0^\infty tdt\ \frac{e^{-2p_n(\ell)\sqrt{t^2+1}}}{(t^2+1)}\tilde{g}^{(0)}(t,a_1(i\omega_n),a_2(i\omega_n)) \tag{8}$$

with

$$\tilde{g}^{(0)}(t,a_1(i\omega_n),a_2(i\omega_n))=2\left[(1+3a_1)(1+3a_2)t^4+2(1+2a_1+2a_2+3a_1a_2)t^2+2(1+a_1)(1+a_2)\right] \tag{9}$$

and

$$\mathcal{A}^{(2)}(\ell)=\frac{k_BT}{32}{\sum_{n=0}^{\infty}}'\Delta_{1,\|}\Delta_{2,\|}\ p_n^4(\ell)\ \int_0^\infty tdt\ \frac{e^{-2p_n(\ell)\sqrt{t^2+1}}}{(t^2+1)}\tilde{g}^{(2)}(t,a_1(i\omega_n),a_2(i\omega_n),\theta) \tag{10}$$

with

$$<C-LeftRelease>\tilde{g}^{(2)}(t,a_1(i\omega_n),a_2(i\omega_n),\theta)=(1-a_1)(1-a_2)(t^2+2)^2 \tag{11}$$

The numerical implementation should be for Eqs. 7-11. For $a_{1,2}$ one invokes the previous definition Eq. 12

$$a_{1,2}(i\omega_n)=\frac{2\Delta_\perp^{(1,2)}(i\omega_n)}{\Delta_\|^{(1,2)}(i\omega_n)}=2\frac{(\epsilon^c{}_\perp{}^{(1,2)}(i\omega_n)-\epsilon_m(i\omega_n))\epsilon_m(i\omega_n)}{(\epsilon^c{}_\perp{}^{(1,2)}(i\omega_n)+\epsilon_m(i\omega_n))(\epsilon^c{}_\|{}^{(1,2)}(i\omega_n)-\epsilon_m(i\omega_n))} \tag{12}$$

where $\epsilon^c{}_\perp{}^{(1,2)}$, $\epsilon^c{}_\|{}^{(1,2)}$ are the perpendicular, parallel components of the dielectric response functions of the two cylinders and ϵ_m is the same for the medium in between. All these quantities are of course frequency dependent. The n summation is over the Matsubara frequencies, $\zeta_n=2\pi nk_BT/\hbar$, where n is an integer and the $n=0$ term is counted with a weight $1/2$. At room temperature the Matsubara frequencies are a multiple of 2.4×10^{14} s^{-1}.

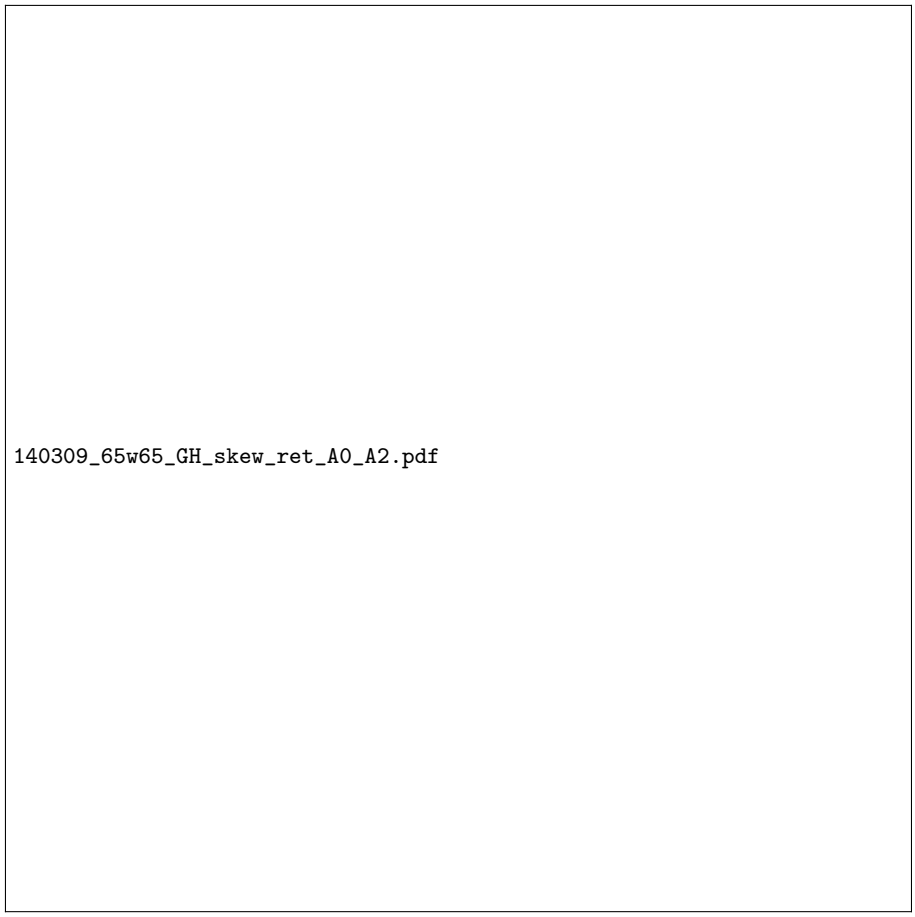

FIG. 10: A sketch of the system of interest (the two cylinders). The quantities describing the geometry of the system are denoted, together with the logitudinal and transverse directions of cylinder in the left half-space (1). The skew angle θ is about an axis normal to the planar boundary defining the limits of each half-space.

TABLE I: Hamaker coefficents for perpendiuclar, retarded formulation at intersurface distance of 1 nm

Case	Method#1	Method#2	Method#3
1	50	837	970
2	47	877	230
3	31	25	415
4	35	144	2356
5	45	300	556

IV. PARALLEL CYLINDERS

The interaction free energy *per unit length*, $g(\ell)$, between two parallel cylinders is given by the Abel transform (see e.g. Ref. **?** , pp 233-235)

$$\frac{d^2\mathcal{G}(\ell,\theta=0)}{d\ell^2} = N_1 N_2 \int_{-\infty}^{+\infty} g(\sqrt{\ell^2+y^2})\; dy. \tag{13}$$

A. Fully retarded

As before, we introduce $p_n^2 = \epsilon_m(i\omega_n)\frac{\omega_n^2}{c^2}\ell^2$, $u = Q\ell$ and $y \longrightarrow y/\ell$. This allows us to rewrite the above integrals as

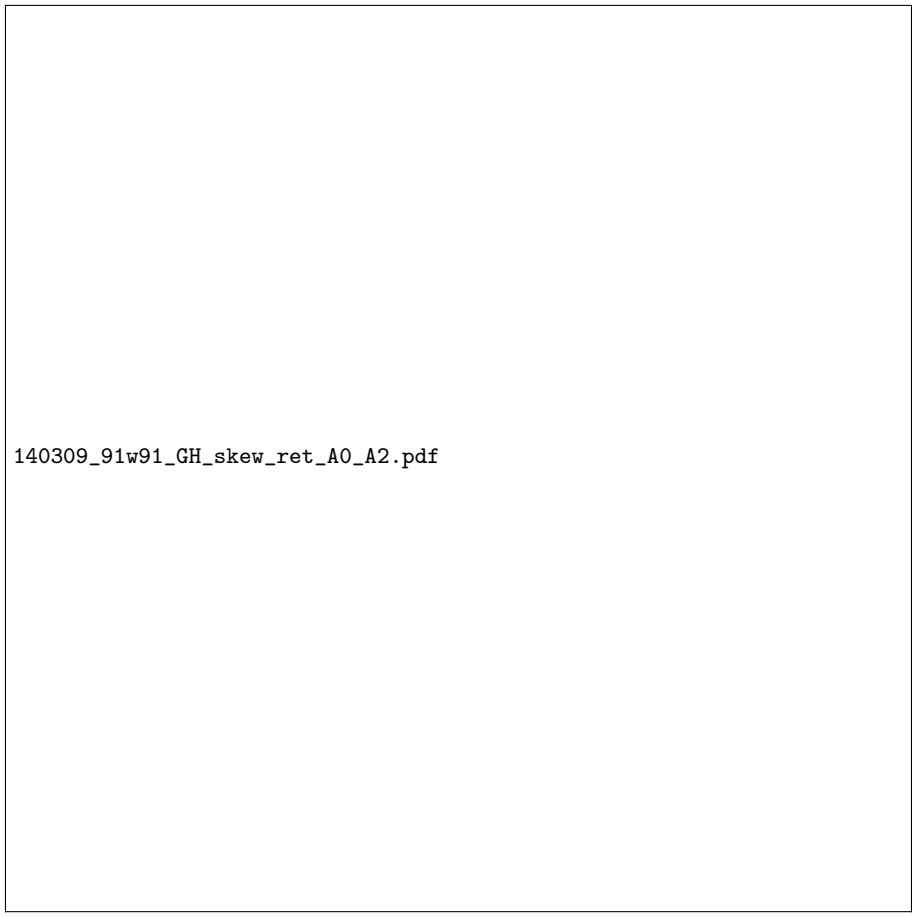

FIG. 11: A sketch of the system of interest (the two cylinders). The quantities describing the geometry of the system are denoted, together with the logitudinal and transverse directions of cylinder in the left half-space (1). The skew angle θ is about an axis normal to the planar boundary defining the limits of each half-space.

TABLE II: Hamaker coefficents, retarded formulation: perpendiuclar cylinders in water, intersurface distance = 1 nm

CNT	$\mathcal{A}^0$ [zJ]	$\mathcal{A}^2$ [zJ]
[6,5]	105.46	0.96
[9,0]	semi-metal; in progress	
[9,1]	93.56	1.56
[9,0]	semi-metal; in progress	
[29,0]	17.73	0.41

$$g(\ell) = -\frac{k_B T}{32}\frac{R_1^2 R_2^2}{\ell^5}{\sum_{n=0}^{\infty}}' \Delta_{1,\parallel}\Delta_{2,\parallel}\int_1^{+\infty}\frac{dy}{\sqrt{y^2-1}}\int_0^{\infty} u du\ \frac{e^{-2y\sqrt{u^2+p_n^2}}}{(u^2+p_n^2)^{1/2}}\ h(a_1(i\omega_n), a_2(i\omega_n), u, p_n^2), \tag{14}$$

and

$$\begin{aligned} h(a_1(i\omega_n), a_2(i\omega_n), u, p_n^2) \ &= \ 2\left[(1+3a_1)(1+3a_2)u^4 + 2(1+2a_1+2a_2+3a_1a_2)u^2p_n^2 + 2(1+a_1)(1+a_2)p_n^4\right] + \\ &\quad (1-a_1)(1-a_2)(u^2+2p_n^2)^2. \end{aligned} \tag{15}$$

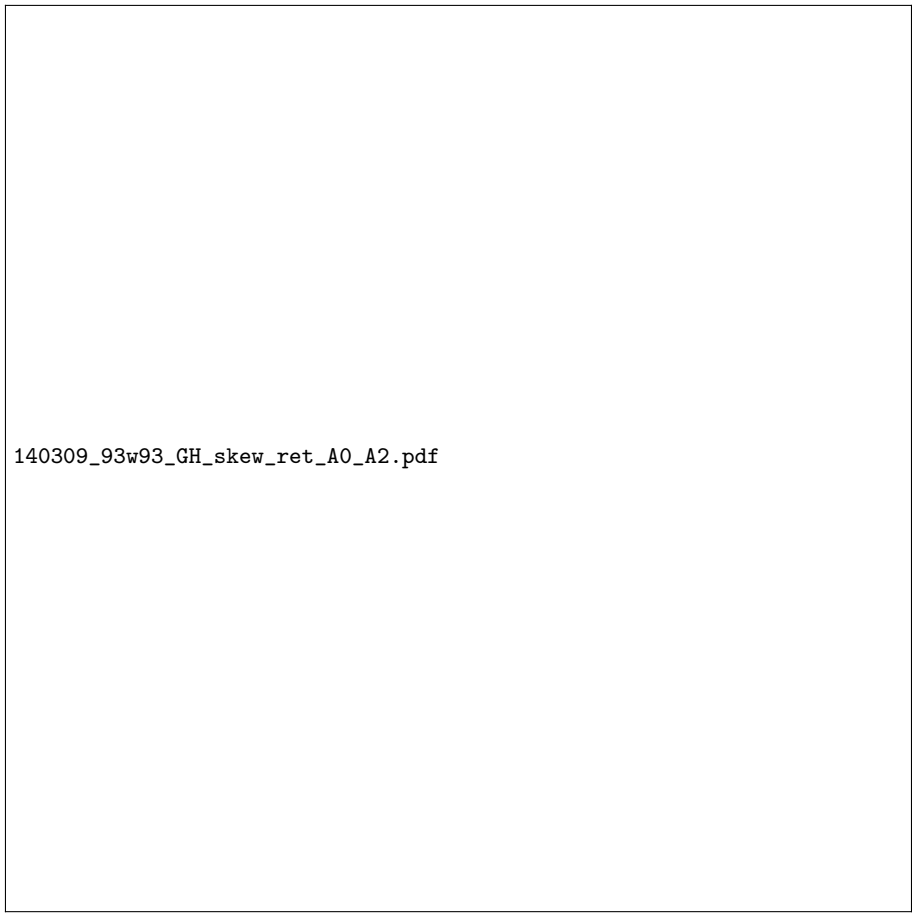

FIG. 12: A sketch of the system of interest (the two cylinders). The quantities describing the geometry of the system are denoted, together with the logitudinal and transverse directions of cylinder in the left half-space (1). The skew angle θ is about an axis normal to the planar boundary defining the limits of each half-space.

TABLE III: Hamaker coefficents, non-retarded formulation: perpendiuclar cylinders in water

CNT	$\mathcal{A}^0$ [zJ]	$\mathcal{A}^2$ [zJ]
[6,5]	126.80	1.16
[9,0]	semi-metal; in progress	
[9,1]	112.22	1.87
[9,3]	semi-metal; in progress	
[29,0]	20.93	0.49

We now again transform this result into a form that is suitable for computation and numerical implementation. Rewriting Eq. 14 as

$$\boxed{g(\ell) = -\frac{3(\pi R_1^2)(\pi R_2^2)}{8\pi\ \ell^5}\mathcal{A}(\ell),} \tag{16}$$

we introduced the Hamaker coefficient

$$\mathcal{A}(\ell) = \frac{k_B T}{12\pi}{\sum_{n=0}^{\infty}}' \Delta_{1,\parallel}\Delta_{2,\parallel}\int_1^{+\infty}\frac{dy}{\sqrt{y^2-1}}\int_0^{\infty} udu\ \frac{e^{-2y\sqrt{u^2+p_n^2(\ell)}}}{(u^2+p_n^2(\ell))^{1/2}}\ h(a_1(i\omega_n), a_2(i\omega_n), u, p_n^2(\ell)) \tag{17}$$

with $h(a_1(i\omega_n), a_2(i\omega_n), u, p_n^2(\ell))$ defined in Eq. 15. This result is simpler then in the skewed case becasue it does not contain any angle dependence. In general $\mathcal{A}(\ell)$ can not be written in terms of $\mathcal{A}^{(0)}(\ell)$ and $\mathcal{A}^{(2)}(\ell)$ of the skewed cylinders.

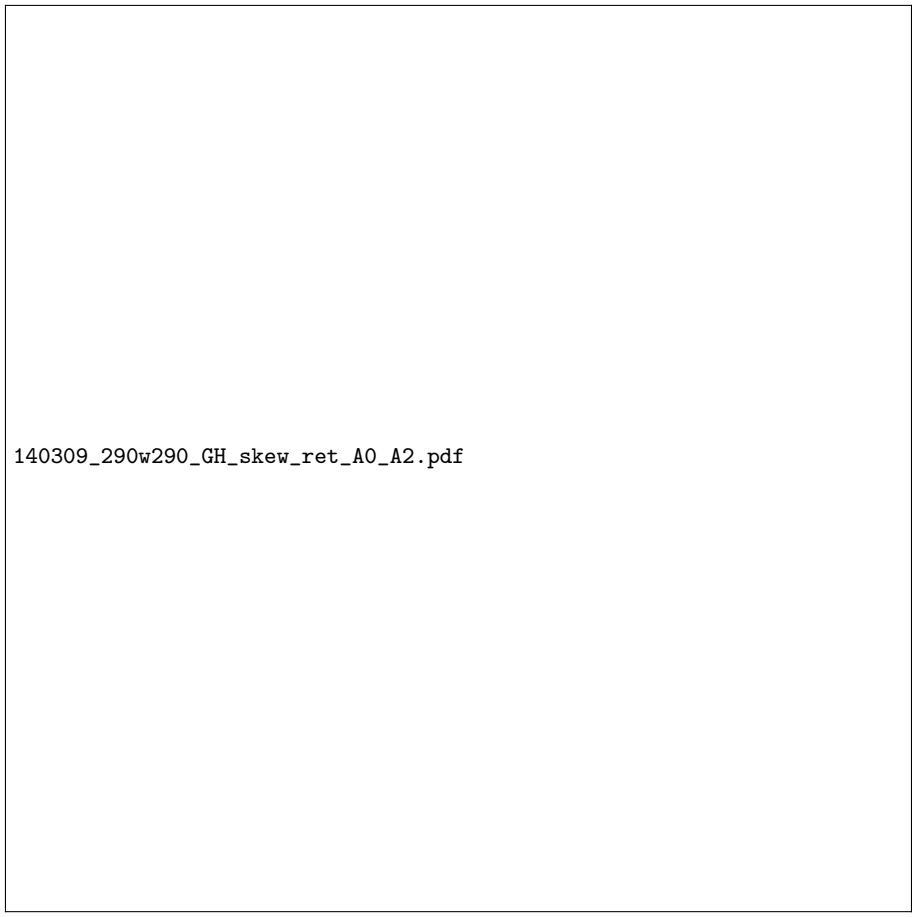

FIG. 13: A sketch of the system of interest (the two cylinders). The quantities describing the geometry of the system are denoted, together with the logitudinal and transverse directions of cylinder in the left half-space (1). The skew angle θ is about an axis normal to the planar boundary defining the limits of each half-space.

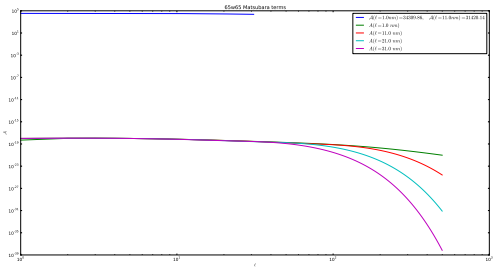

FIG. 14: A sketch of the system of interest (the two cylinders). The quantities describing the geometry of the system are denoted, together with the logitudinal and transverse directions of cylinder in the left half-space (1). The skew angle θ is about an axis normal to the planar boundary defining the limits of each half-space.

TABLE IV: Hamaker coefficents for parallel cylinders, retarded formulation at intersurface distance of 1 nm

CNT	$\mathcal{A}^0$ [zJ]	$3\mathcal{A}^2$ [zJ]
[6,5]	105.46	0.96
[9,0]	addressing	monopole flucuations
[9,1]	93.56	1.56
[9,3]	addressing	monopole flucuations
[29,0]	17.73	0.41

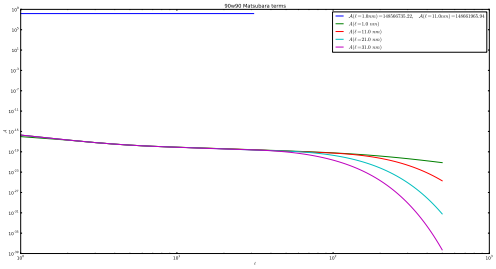

FIG. 15: A sketch of the system of interest (the two cylinders). The quantities describing the geometry of the system are denoted, together with the logitudinal and transverse directions of cylinder in the left half-space (1). The skew angle θ is about an axis normal to the planar boundary defining the limits of each half-space.

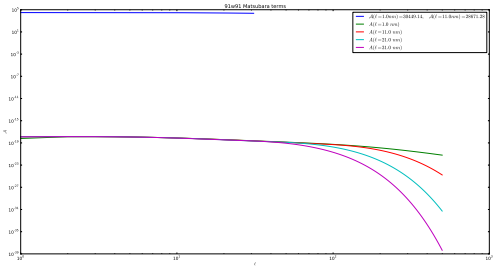

FIG. 16: A sketch of the system of interest (the two cylinders). The quantities describing the geometry of the system are denoted, together with the logitudinal and transverse directions of cylinder in the left half-space (1). The skew angle θ is about an axis normal to the planar boundary defining the limits of each half-space.

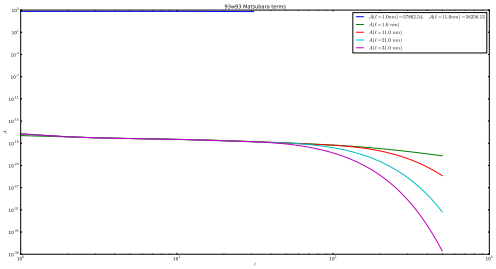

FIG. 17: A sketch of the system of interest (the two cylinders). The quantities describing the geometry of the system are denoted, together with the logitudinal and transverse directions of cylinder in the left half-space (1). The skew angle θ is about an axis normal to the planar boundary defining the limits of each half-space.

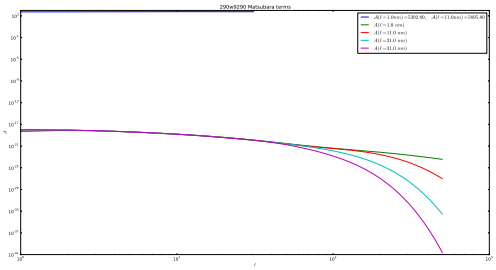

FIG. 18: A sketch of the system of interest (the two cylinders). The quantities describing the geometry of the system are denoted, together with the logitudinal and transverse directions of cylinder in the left half-space (1). The skew angle θ is about an axis normal to the planar boundary defining the limits of each half-space.

TABLE V: Hamaker coefficents for parallel cylinders, Non-retarded formulation

CNT	$\mathcal{A}^0$ [zJ]	$3\mathcal{A}^2$ [zJ]
[6,5]	105.46	0.96
[9,0]	addressing	monopole flucuations
[9,1]	93.56	1.56
[9,3]	addressing	monopole flucuations
[29,0]	17.73	0.41